Chapter 11

Effect of Climate Change on Spatio-Temporal Variability and Trends of Evapotranspiration, and Its Impact on Water Resources Management in The Kingdom of Saudi Arabia

Mohammad Elnesr and Abdurrahman Alazba

Additional information is available at the end of the chapter

http://dx.doi.org/10.5772/54832

1. Introduction

Recently, climate change is receiving much attention. Changes in the world's climate have significant effect on water resources which affect the livelihood of people especially in hyper arid regions such as the Kingdom of Saudi Arabia (KSA). The KSA suffers an enduring water shortage problem, despite the fact that the agricultural activities consume up to 90% of the water amount in the Kingdom. Reference Evapotranspiration (ETo) is an agro-climatic property that involves temperature, humidity, solar radiation, and wind speed. Identifying changes in ETo can also help in future planning of agriculture-water projects and identify lower and higher ETo zones for proper planning and management of agricultural projects in arid regions.

1.1. Water resources and climate change

Water shortage is a swelling problem in the arid and semi-arid regions. Affected by its geographic location and its climate, the Kingdom of Saudi Arabia (KSA) suffers a severe water deficit. Even rain, which is the only renewable water source, comes in flash short duration storms of high intensity and most of it vanishes to evaporation. Thus, almost all agriculture of the kingdom is irrigated. Irrigation water, though, consumes 80 to 88 % of the total water consumption (Abu-Ghobar, 2000; Abderrahman, 2001). In addition to these water scarcity conditions, but it seems getting scary by the effects of climate change on the hydrological cycle and water supply. The quantity of irrigation water is determined initially by identifying the reference evapotranspiration (ETo). Several researches was conducted to detect climate changes, trends and variability in various parts of the world using some climate parameters such as air temperature, rainfall depth, ETo, and pan evapotranspiration ETp (Shwartz and Randall, 2003; Garbrecht, et al., 2004; Hegerl, et al., 2007; Fu, et al., 2009; Hakan, et al., 2010; Elnesr and Alazba, 2010; Elnesr et al., 2010a; and Elnesr et al. 2010b). The ETo parameter has a special importance because it combines changes in many other climate parameters including temperature, radiation, humidity, and wind speed. It has, however, direct influence on hydrologic water balance, irrigation and drainage canal design, reservoir operation, potentials for rain-fed agricultural production, and crop water requirements (Dinpashoh, 2006).

1.2. Climate change effect on evapotranspiration worldwide

Several studies conducted in North America have shown that some climate parameters are on the rise including ETo (Fehrman, 2007; Garbrecht et al., 2004; Szilagyi, 2001). Fehrman, 2007 found an increasing trend in ETo over the Mississippi area and that most of ETo increase can be attributed to the increase in July. He also found that the rate of ETo increase was 0.29 mm/years when his study period extended from 1940 to 1999 compared to 0.88 mm/year when the study period was limited to 1950 to 1999 records. The accelerated ET over North America is presumed to be due to a rise in temperature over the past century (Myeni et al. 1997, Milly and Dunne 2001). In the contrary ETo and pan evaporation has shown to decrease in China (Thomas, 2000, Liu et al., 2004) and at a rate of 1.19 mm/year (Song et al., 2010) despite the rise in maximum daily temperature. In the Tibetan Plateau ETo decreases as well at a rate of 1.31 mm/year or 2.0% of the annual total evapotranspiration (Shenbin et al., 2006). The decrease in ETo has been attributed to the decrease in wind speed and net radiation. In another study Gao et al., (2007) found that the actual evapotranspiration had a decreasing trend in most of the eastern part of china and there was an increasing trend in the western and the northern parts of northeast China and that the change in precipitation played a key role for the change of estimated actual evapotranspiration. Similar negative trends in pan evaporation were found in 24 out of 27 observation stations in a 19-year study in Thailand (Tebakari et al., 2005). In India, a significant decreasing trend was found in ETo all over the Indian plateau during the past 40 years, which was mainly caused by a significant increase in the relative humidity and a consistent significant decrease in the wind speed throughout the country (Bandyopadhyay et al., 2009). In Australia, Roderick and Farquhar (2004) found a decreasing trend in pan evaporation and conclude that Australia is becoming less arid. However, there is enough evidence now that a decrease in pan evaporation is an indicator to an increase in actual evaporation. This is what known now as the evaporation paradox (Hobbins et al., 2004).

Some researchers developed a hypothetical scenario to study the effect of possible increase on temperature over the ETo and subsequently on water supply. A study conducted by Abderrahman et al. (1991) concluded that in the KSA, a 1°C increase in temperature would increase ETo from 1 to 4.5%. In another study, that includes selected cities in KSA, United Arab Emirates and Kuwait, Abderahman and Al-Harazin (2003) concluded that an increase in temperature by 1°C would increase ETo over these area by a maximum of 20%. In general, studies involving ETo calculation seemed to be more limited worldwide compared to other climate parameters. In the other hand, regarding other climatic parameters, Hakan et al. (2010) reported an increasing trend in temperature and ETo in most of stations they analyzed in Turkey using Mann-Kendall analysis. Cohen and Stanhill, (1996) studied rainfall changes in the Jordan Valley/Jordan and found a tangible but insignificant decrease at a rate of -0.47 and -0.16 mm/year for two different stations. Similar conclusions were observed by Al-Ansari et al (1999) who observed a general decrease in rainfall intensity. Smadi (2006), and Smadi and Zghoul (2006) found a prompt shift in rainfall and temperature in Jordan. ElNesr et al (2010b) concluded that the Saudi Arabia and the Arabian Peninsula are suffering from a considerable warming trend form year 1980 to 2008. Still, Elnesr et al. (2010a) concluded that the percentage land area with annual ET_o>4000 mm increased from about 20% to 40% in the period they studied. On the other hand, lower ET_o values, less than 3600 mm, contracted from about 30% to 12%.

1.3. Objective of the study

This study aims to trace the ETo values over time throughout all the area of the Saudi Arabia, then to quantify the future of water demand according to the ETo trends

2. Material and methods

2.1. Geography of the Saudi Arabia

Saudi Arabia is the largest country of the Arabian Peninsula; it occupies about 80% of its area (Wynbrandt, 2004). The country lies between latitudes 16°21'58''N, and 32°9'57''N, and longitudes 34°33'48''E and 55°41'29''E, as illustrated in Fig. 1. Saudi Arabia has a desert dry climate with high temperatures in most of the country. However, the country falls in the tropical and subtropical desert region. Winds reaching the country are generally dry, and almost all the area is arid. Because of the aridity and the relatively cloudless skies, there are great extremes in temperature, but there are also wide variations between the seasons and regions (AQUASTAT, 2008).

2.2. Evapotranspiration calculation

Evapotranspiration was calculated using Food and Agricultural Organization (FAO) Penman- Monteith (PM) procedure, FAO 56 method, presented by Allen et al. (1998). In this method, ETo is expressed as follows:

$$ET_o = \frac{0.408\Delta\left(R_n - G\right) + \dfrac{900}{\left(T_a + 273\right)}\gamma U_2\left(e_s - e_a\right)}{\Delta + \gamma\left(1 + 0.34U_2\right)} \quad (1)$$

where ET_o is the daily reference evapotranspiration [mm day-1], R_n is the net radiation at the crop surface [MJ m-2 day-1], G is the soil heat flux density [MJ m-2 day-1], T_a is the mean daily air temperature at 2 m height [°C], U_2 is the wind speed at 2 m height [m s-1], e_s: saturation vapor pressure [kPa], e_a: actual vapor pressure [kPa], Δ is the slope of vapor pressure curve [kPa °C^{-1}], and γ is the psychometric constant [kPa °C^{-1}].

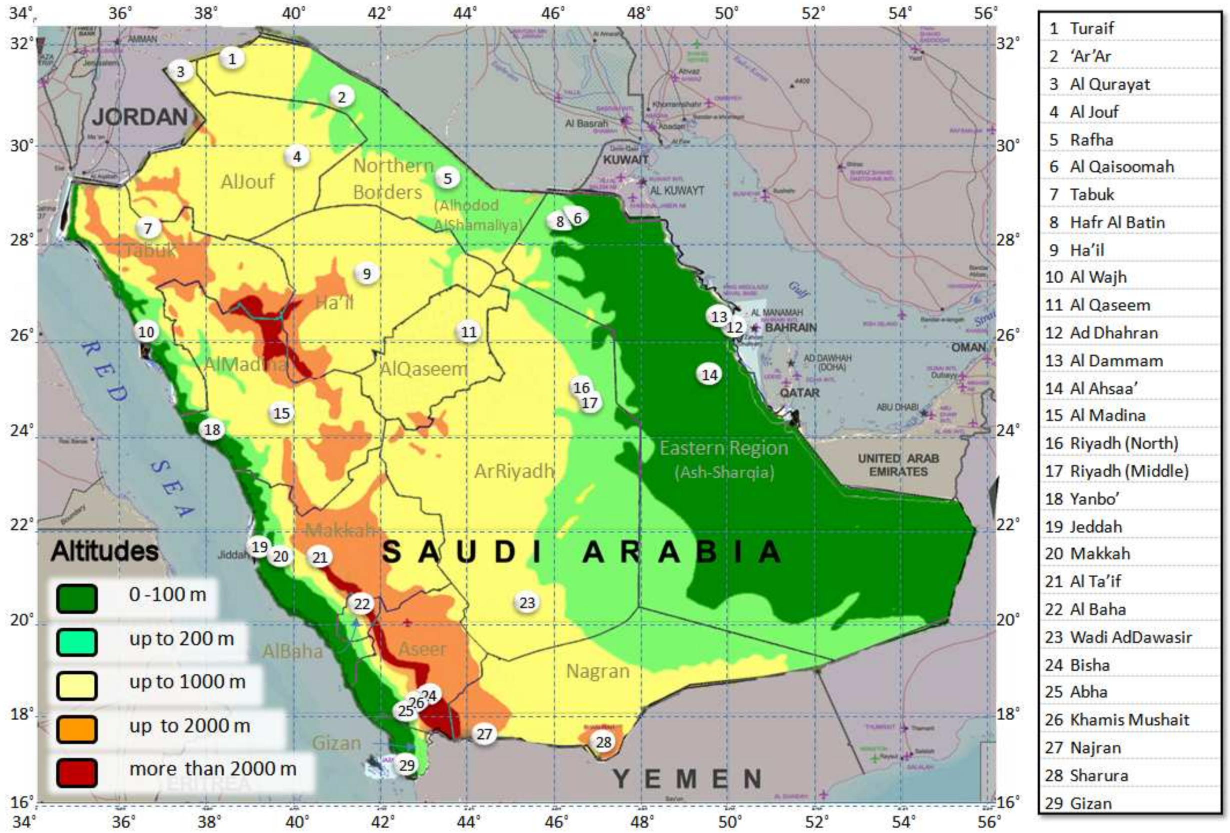

Figure 1. Geographic map of Saudi Arabia, showing 13 districts and 29 meteorological stations. *Base map Src: NIMA (2003). Districts Src: MOMRA (2007), Topography Src: Albakry et.al. (2010)*

The measured meteorological data available were T_a, Relative humidity (RH) and U_2 whereas soil heat flux (G) was taken equal to zero, (Allen et al, 2005). The slope of the saturation vapor pressure curve (Δ) is computed by the following equation as in Murray (1967):

$$\Delta = \frac{4098 \times e_o\left[T_a\right]}{\left(T_a + 237.3\right)^2} \tag{2}$$

where $e_o\left[T_a\right]$ is calculated according to (Tetens, 1930):

$$e_o\left[T\right] = 0.611 \exp\left(\frac{17.27\, T}{T\ + 237.3}\right) \tag{3}$$

The net radiation R_n was estimated as the difference between the net short wave incoming radiation R_{ns} and the net long wave outgoing radiation Rnl. The calculation of R_{ns}, and R_{nl}, followed the procedures outlined in Allen et al. (1998) and Doorenbos and Pruitt (1977). All radiation was computed in daily energy flux units (MJ m^{-2} day^{-1}). Allen et al (1998) reported a validated formula to calculate the incoming solar radiation R_s from air temperature difference:

$$R_s = c\,R_a \sqrt{T_x - T_n} \tag{4}$$

where R_a: extraterrestrial radiation [MJ m-2 d-1], c: an adjustment coefficient =0.19 for coastal stations and 0.16 for inland stations; T_n: minimum dry bulb air temperature [°C], T_x: maximum dry bulb air temperature [°C]. The psychometric constant γ is evaluated as:

$$\gamma = 0.00163 \frac{P}{\lambda} \tag{5}$$

where P : atmospheric pressure [kPa], λ: latent heat flux [MJ kg-1]. The atmospheric pressure is expressed as in Burman et al. (1987)

$$P = 101.3 \left(\frac{293 - 0.0065z}{293} \right)^{5.26} \tag{6}$$

where z: altitude [m]. The latent heat λ depends on the average temperature, Eqn(7) , while it can be taken as an approximate value of 2.45 as reported by Harrison (1963) for T_a=20 °C. In the current study, we chose to calculate the latent heat using Eqn(7) .

$$\lambda = 2.5 - 0.00236\,T_a \tag{7}$$

The saturation vapour pressure, e_s, and actual vapour pressure, e_a, are calculated according to Allen et al (2005) as:

$$e_s = 0.5\left(e_o\left[T_n\right] + e_o\left[T_x\right]\right) \tag{8}$$

$$e_a = 0.005\left(RH_x e_o\left[T_n\right] + RH_n e_o\left[T_x\right]\right) \tag{9}$$

where RH_x, RH_n: maximum and minimum relative humidity [%] respectively.

The average daily ET_o in a specific month was calculated by taking the arithmetic average of the daily values in that month. The summation of all ET_o daily values in a year for a station will give the total annual ET_o for that station.

2.3. Climatic data source and description

Basic climatic data were taken from the Presidency of Meteorology and Environment in KSA, the official climate agency in the country. The data set is the most accurate one in KSA and used by all other governmental and academic agencies for climate research and prediction. Weather stations are equipped with up-to-date monitoring devices and subjected to regular inspection and replacement for defected devices (personal communication with the Presidency of Meteorology and Environment). Data represents 29 meteorological stations as shown in Fig. 1. These stations represent all the 13 districts of the KSA. The data covers 29 years of daily meteorological records for 20 stations, 24 years for 6 stations, and 3 stations with less than 20 years as shown in Table 1. All of the data ends in 2008 and started at 1980 and 1985 for the 29 and 24 years logging.

District	Station		Station coordinates			Recroded Years**
	ID	Name	Latitude	Longitude	Altitude	
			Deg. N.	Deg. East	m	
Northern Borders	1	Turaif	31.41	38.4	818	29
	2	Arar	31.00	41.00	600	29
	5	Rafha	29.38	43.29	447	29
AlJouf	3	Guraiat*	31.50	37.50	560	4
	4	Al Jouf	29.47	40.06	671	29
Tabuk	7	Tabuk	28.22	36.38	776	29
	10	Wejh	26.12	36.28	21	29
Ha'il	9	Hail	27.26	41.41	1013	29
AlQaseem	11	Gassim	26.18	43.46	650	29
Eastern Region	6	Qaisumah	28.32	46.13	358	29
	8	Hafr Al-Batin	28.20	46.07	360	19
	12	Dhahran	26.16	50.10	17	29
	13	Dammam*	26.42	50.12	1	9
	14	Ahsa	25.30	49.48	179	24
Riyadh	16	Riyadh North	24.42	46.44	611	24
	17	Riyadh Middle	24.63	46.77	624	29
	23	W-Dawasir	20.50	45.16	652	24
Madina	15	Madina	24.33	39.42	636	29
	18	Yenbo	24.09	38.04	6	29
Makkah	19	Jeddah	21.30	39.12	17	29
	20	Makkah	21.40	39.85	213	24
	21	Taif	21.29	40.33	1454	29
Baha	22	Baha	20.30	41.63	1652	24
Aseer	24	Bisha	19.59	42.37	1163	29
	25	Abha	18.14	42.39	2093	29
	26	Khamis Mushait	18.18	42.48	2057	29
Nagran	27	Nejran	17.37	44.26	1210	29
	28	Sharurrah	17.47	47.11	725	24
Gizan	29	Gizan	16.54	42.35	3	29

*: Stations having less than 10 years of data.
**: average error ratio in data recording is less than 0.7% including missing records if any.

Table 1. Geographical information of the meteorological stations included in this study.

2.4. Data grouping and contouring

After correction the data sets, daily ETo values were calculated for each station, then aggregated to annual and monthly values. Annual ETo value (mm/year) for each station was calculated by summation of the daily ETo for the entire year. On the other hand, the monthly average ETo value was calculated by taking the average of the daily ETo values during each month.

Evapotranspiration data were graphically represented by contour maps irrespective of stations altitude. Analysis of ET variations with stations' altitude for each of the 30 years under study revealed no trends. Other researchers have also found no correlation between ET and station altitude in China (Thomas, 2000). Contour maps present clearly zones of common ET values as well as clarify vividly ET differences between zones and viability a long months or years. This approach has also been adopted by other researchers to study ET variability in China (Thomas, 2000; Shenbin et al., 2006).

Data was arranged in three columns format namely, longitude, latitude, and ETo. Each set of data was gridded separately using the ordinary point-Kriging method which estimates the values of the points at the grid nodes (Abramowitz and Stegun, 1972, and Isaaks and Srivastava, 1989). This procedure is used by SURFER™ Software which has been used in our calculations. The resulted grid was blanked outside the political borders of the KSA. The political borders' information of the KSA was grabbed from electronic map of NIMA (2003). The electronic map was digitized and converted to DMS geographic coordinate system. The blanked grid was plotted as a contour map using Surfer™ 8.0 software (Surfer, 2002). Sample plots for the average daily ET_o during a month, June in this case and the ET_o, in a year, 1991 in this case, is shown in Figure (#2a, b), respectively, where darker areas represent smaller magnitudes of ET_o.

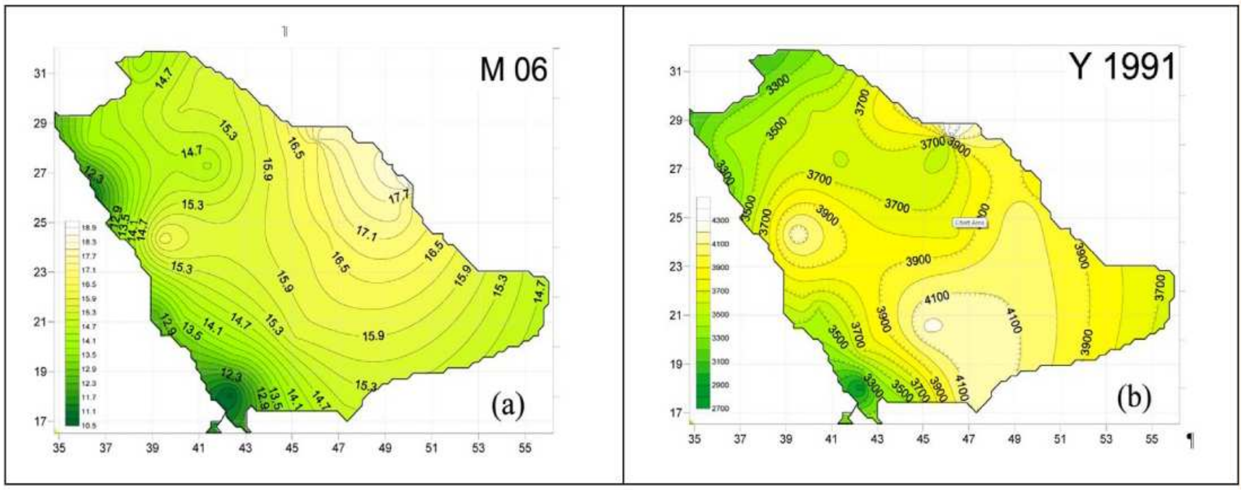

Figure 2. Sample contour map of daily and annual evapotranspiration in the KSA.
(a): average daily evapotranspiration for the month of June over 30 years period (mm/d). (b): annual evapotranspiration of the year 1991 (mm/y)

All of the data are daily values, the obtained climatic data records were carefully inspected for missing and erroneous reading. Very few errors were found, (median value of 00.45%). Errors were classified into four categories: Errors because of mistaken extreme values such as a relative humidity exceeds 100% or below 0%. Illogical errors such as the recorded maximum daily temperature (T_x) was less than the minimum daily temperature (T_n) in the same day, or if $T_x = T_n$. Missing values; i.e. T_x is present but T_n is missing. Recording an error-indication number (like 999 or 777) if the sensor is not functioning. On analyzing the data record, any value contains one or more errors was considered missing record unless the missing record could be predicted with minimal error, i.e. if the average temperature (Ta) is missing while T_x and T_n are logged with no errors; in this case Ta = $(T_x + T_n)/2$. However, the amount of missing data in the recorded period could be considered negligible in most of the stations, where the average amount of missing data is 0.78%.

2.5. Non-parametric trend analysis methods

2.5.1. Mann-kendall test

The Mann-Kendall test is a non-parametric test used for identifying trends in time series data. The test compares the relative magnitudes of sample data rather than the data values themselves Both Kendall tau coefficient (τ) and Mann-Kendall coefficient (s) are nonparametric statistics used to find rank correlation. Kendall (τ) is a ratio between the actual rating score of correlation, to the maximum possible score. To obtain the rating score for a time series, the dataset is sorted in ascending order according to time, and then the following formula is applied:

$$s = \sum_{j=1}^{j=n-1} \sum_{i=j+1}^{i=n} \mathrm{Sign}\left(x_i - x_j\right) \tag{10}$$

where s: the rating score (also called the Mann-Kendall sum); x: the data value; i and j: counters; n: number of data values in the series; Sign is a function having values of +1, 0, or -1 if (x_i-x_j) is positive, zero, or negative, respectively. According this formula, the maximum value of s is:

$$s_{\max} = \frac{1}{2} n\left(n-1\right) \tag{11}$$

Hence, the Kendall (τ) is calculated as:

$$\tau = \frac{s}{s_{\max}} \tag{12}$$

A positive value of s or τ is an indicator of an increasing trend, and a negative value indicates a decreasing trend. However, it is necessary to compute the probability associated with s or τ and the sample size, n, to quantify the significance of the trend statistically. Kendall and Gibbons (1990) introduced a normal-approximation test that could be applied on datasets of more than ten values with s variance (σ^2):

$$\sigma^2 = \frac{1}{18} n(n-1)(2n+5) - CF_R \tag{13}$$

$$CF_R = \frac{1}{18} \sum_{k=1}^{g} m_k (m_k - 1)(2m_k + 5) \tag{14}$$

where CFR: repetition correction factor, to fix the effect of tied groups of data (when some of the data values appear more than one time in the dataset, this group of values are called a tied group); *g*: number of tied groups; *k*: a counter; m: number of data values in each tied group. Then normal distribution parameter (called the Mann-Kendall statistic, *Z*) is calculated as follows:

$$Z = \begin{cases} \frac{1}{\sigma}(s-1) & \rightarrow \quad s > 0 \\ 0 & \rightarrow \quad s = 0 \\ \frac{1}{\sigma}(s+1) & \rightarrow \quad s < 0 \end{cases} \tag{15}$$

The last step is to find the minimum probability level at which the parameter *Z* is significant, this could be found using two-tailed *t* statistical Tables or as mentioned by Abramowitz and Stegun *(1972):*

$$\alpha_{min} = \left(b_0 \, e^{-0.5Z^2}\right) \sum_{q=1}^{q=5} b_q \cdot \left(1 + b_6 \text{ ABS}(Z)\right)^{-q} \tag{16}$$

where αmin: Minimum level of significance; q: counter; bx: constants: b0= 0.3989, b1= 0.3194, b2= -0.3566, b3= 1.7814, b4= -1.8213, b5= 1.3303, b6= 0.2316, ABS(Z): the absolute value of Z. Kendall tau is considered significant when alpha min is less than a specified alpha value, i.e 0.05.

2.5.2. Sen-slope estimator test

Sen's statistic is the median slope of each point-pair slope in a dataset (Sen, 1968). To perform the complete Sen's test, several rules and conditions should be satisfied; the time series should be equally spaced, i.e. the interval between data points should be equal. However, Sen's method considers missing data. The data should be sorted ascending according to time, and then apply the following formula to calculate Sen's slope estimator (Q) as the median of Sen's matrix members.

$$Q = \text{Median}\left\{ \left[\left[\frac{x_i - x_j}{i - j} \right]_{j=1}^{j=n-1} \right]_{i=j+1}^{i=n} \right\} \tag{17}$$

Its sign reflect the trend's direction, while its value reflects how steep the trend is. To determine whether the median slope is statistically different than zero, the variance is calculated using Eqn. (13), to obtain the confidence interval of Q at a specific probability level, e.g 95%. The area (Z) under two-tailed normal distribution curve is calculated at the level (1-α/2), where α=1-confidence level. For example, for a confidence level of 95%, Z should be evaluated at 0.975, hence Z= 1.96. Next, the parameter C_α is calculated as follows:

$$C_\alpha = Z_{1-\alpha/2}\sqrt{\sigma^2} \tag{18}$$

The upper and lower confidence boundaries for Q are then calculated as follows:

$$\begin{aligned} M_u &= \text{int}\left(0.5\left(n_q - C_\alpha\right)\right) \\ M_l &= \text{int}\left(0.5\left(n_q + C_\alpha\right)\right) + 1 \end{aligned} \tag{19}$$

where int() represents the integer value; M_u and M_l are the upper and lower boundaries for Q at 1-α probability level; nq is the number of Sen's matrix members calculated from Equation (17), equal to n_q=n(n-1). The median slope is then defined as statistically different from zero for the selected confidence interval if the zero does not lie between the upper and lower confidence limits.

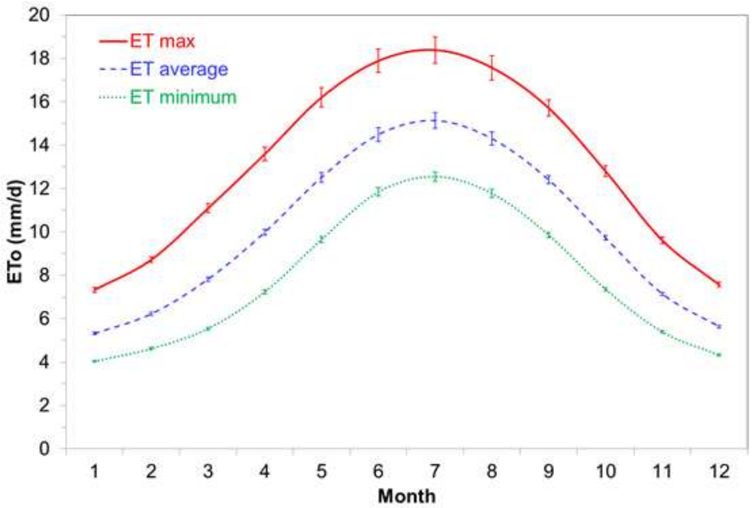

Figure 3. The monthly average ET_o variations during the year in KSA, vertical bars indicate standard deviation values.

3. Results and discussion

The daily ET_o data for each of the studied stations were calculated for the study period. Then we summarize the data on monthly basis to find the average, maximum and minimum values per month for the whole country, Figure 3. The lowest values of ET_o occurred in the winter season, December and January whereas the highest values occurred during summer months; June, July and August. The results showed high variation in ET_o from about 5 mm/day to 15 mm/day in July whereas the absolute minimum and maximum ET_o showed even higher variation and ranged from 3.9 mm/day in January to as high as 18.5 mm/day in July. However, Figure 2 indicates the high variability of climate conditions over Saudi

Arabia, which highlights the major challenge for agricultural development and water resources planning in the country.

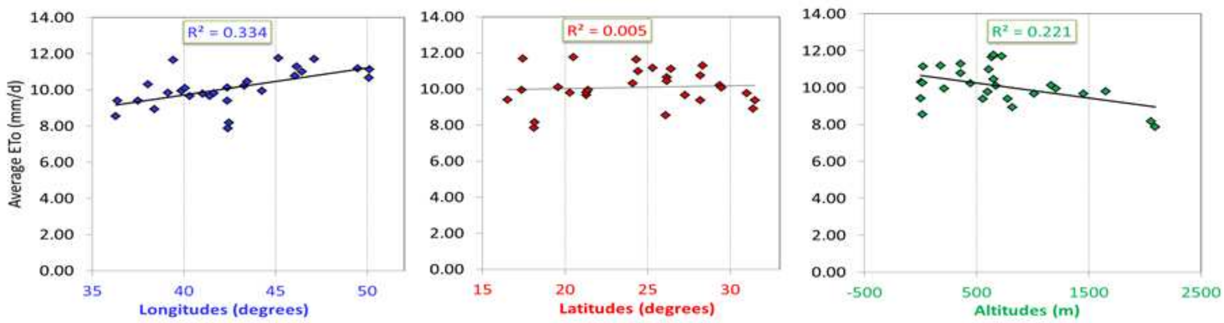

Figure 4. Relationship between the average annual ET_o (mm/d) as related to station altitudes, latitudes, and longitudes.

The variation of ET_o over the area of Saudi Arabia is large, as it should be due to its large surface area and large differences in altitudes. Therefore, the average ET_o values in the study period for the studied stations were plotted with their altitude, latitude and longitudes and the results are shown in Figure 4. As expected ET_o decreased with station altitude as weather stations varied from sea level, Yenbo' and Jeddah stations to as high as 2300 m above sea level in Nejran. Similar relationships were found with temperature and stations altitudes in the study of ElNesr et al., (2010b), which may be a significant reason for rising ET_o values. However, large variabilities were also observed among stations at the sea level suggesting that other factors may have compound effect on ET_o in Saudi Arabia such as the geographic location (latitude and longitude). While latitudes seemed to have no effect on the variability of ET_o, longitudes have tangible effect on it,. ET_o increased steadily with stations longitudes as we travel toward the east. The concentration of oil industries and refineries in the eastern parts of KSA may have affected air temperature, while the nearness to the Arabian Gulf increased the relative humidity, thus leads to raising ET_o in the eastern parts of KSA relative to the other parts.

The changes in ET_o with time was examined by calculating the average daily evapotranspiration (mm/d) over the whole study period of each station, and plotting time series ET_o for the study period, Figure 5. The Figure shows clearly a positive trend of $ET_o$with time during the study period. The ET_o has increased from about 9.6 in 1980 to about 10.4 mm/day in 2008 at a rate of 0.02 mm/day. Regression analysis between ET_o and time has confirmed the positive trend and showed that the slope of the line was 0.020 with $R^2 = 0.50$. However, this relationship was not statistically significant at 95% probability level. Longer period of data analysis is needed to confirm this result. Nevertheless, the present analysis indicates clearly that climate variability is indeed affecting the country and the evapotranspiration demand is increasing with time.

Due to some restrictions in Man-Kendall and Sen's methods, two stations out of the 29 stations were omitted from calculations due to the small number of years they had (less than 10 years); those were stations #3 (Guraiat) and # 13 (Dammam). Mann-Kendall and Sen

Slope statistics were performed on the rest 27 stations on monthly basis to confirm trends direction and test its significance. Two parameters were calculated namely Kendall τ and Sen Slope Q and their confidence limits at 95% and 99% probability level as described in Materials and Methods. A group of selected results is shown in Figure 6 where the parameters of Mann-Kendall and Sen Slope and their significant tests are presented. The Figure represents ET trends in January for four stations, Tabuk, Sharurrah Yenbo, and Hail, showing possible combinations of Mann-Kendall (MK) and Sen Statistic, in addition to their significance under increasing or decreasing ET_o conditions. That is, Figure 6a showing a downtrend with MK and Sen significant at 95% and 99%. Figure 6b showing a downtrend with only MK is significant at 95%. Figure 6c showing an uptrend with all statistics was significant. Figure 6d showing an uptrend with only MK is significant at 95%.

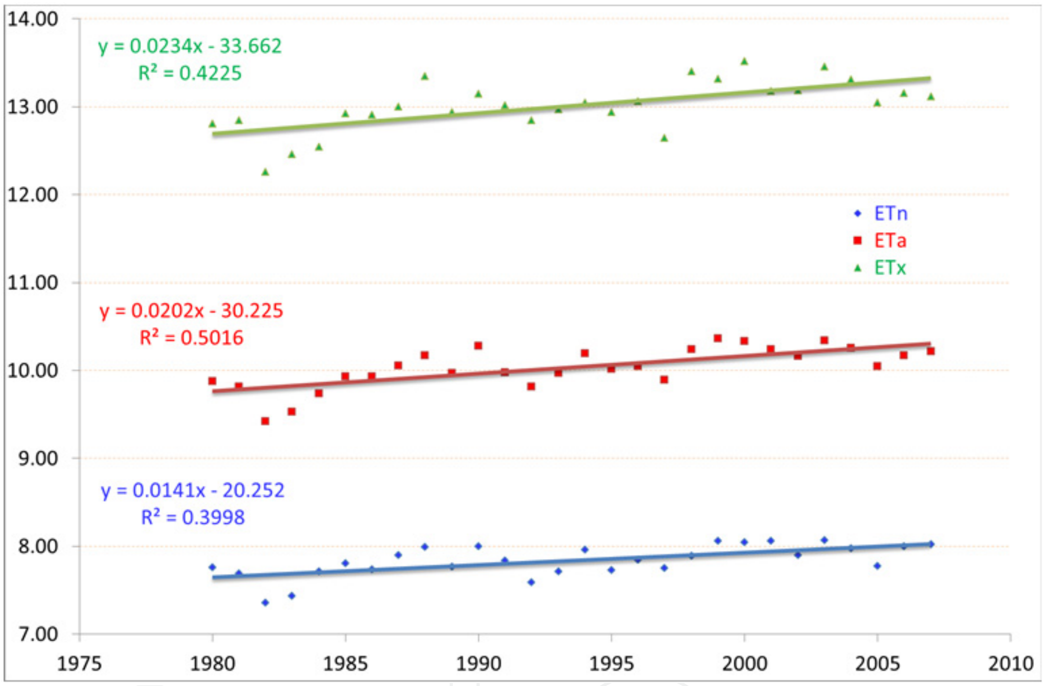

Figure 5. Temporal change of the average, maximum, and minimum ET_o through the study period.

The two tests gave similar results in all of these cases but Sen Slope test were found to be more conservative. A positive sign in τ or Q indicates an increasing trend, Figure 6 C and D while a negative value indicates a decreasing trend, Figure 6 A and B. The significance of τ was tested by comparing the calculated α_{min} with $\alpha = 0.05$ or 0.01 for 95% and 99% confidence level, respectively; $\alpha_{min} < 0.05$ or 0.01. The corresponding significant test for Q was carried out by calculating its confidence intervals at 95% and 99% indicated by ($Q^{95\%}_{\min}$, $Q^{95\%}_{\max}$) and ($Q^{99\%}_{\min}$, $Q^{99\%}_{\max}$), respectively. If the two limits have similar sign, then the calculated Sen Slope Q value is confirmed not to be zero and therefore the slope is significantly different from zero, indicating a positive or negative trend for $+Q$ or $-Q$, respectively.

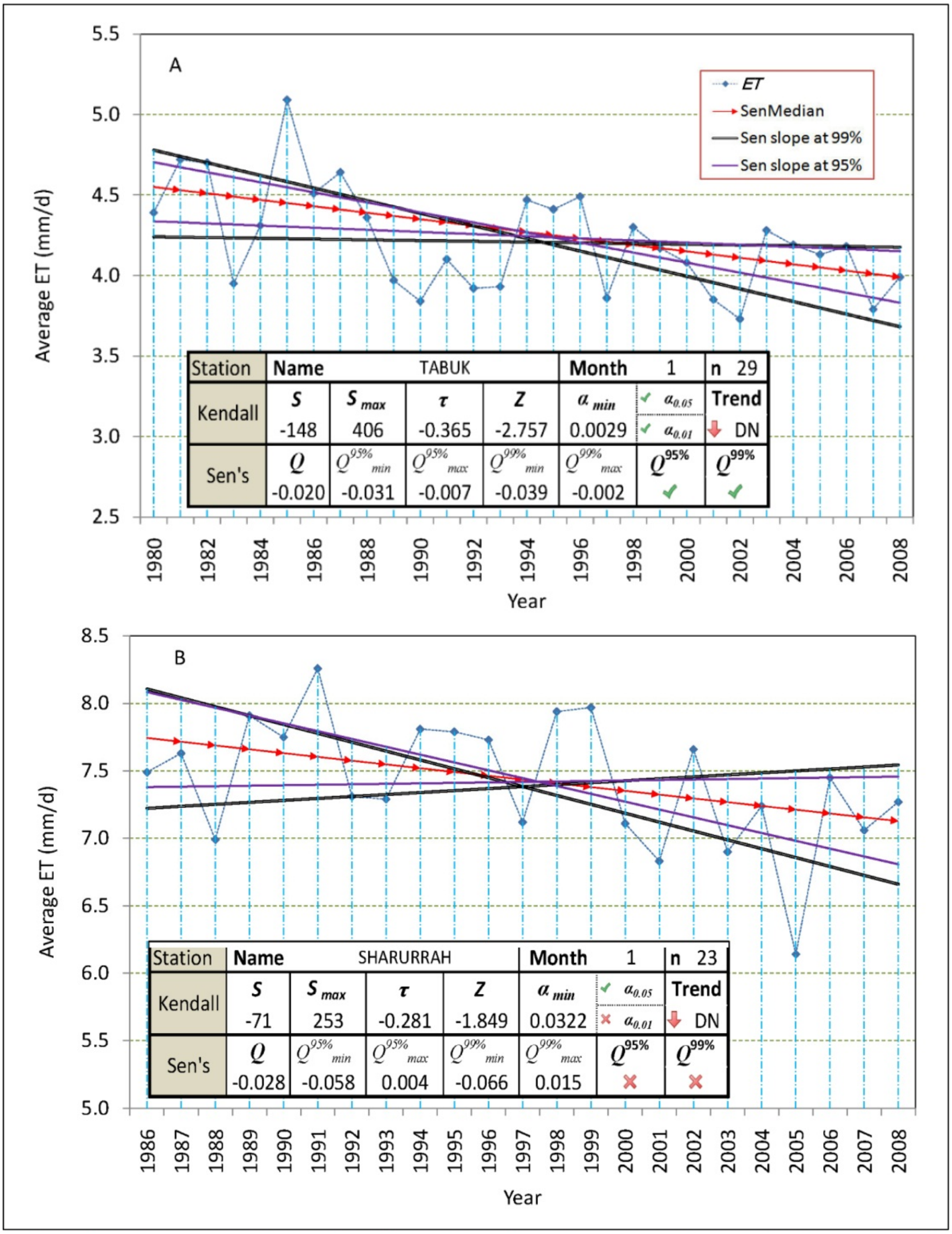

to be continued in the next page.

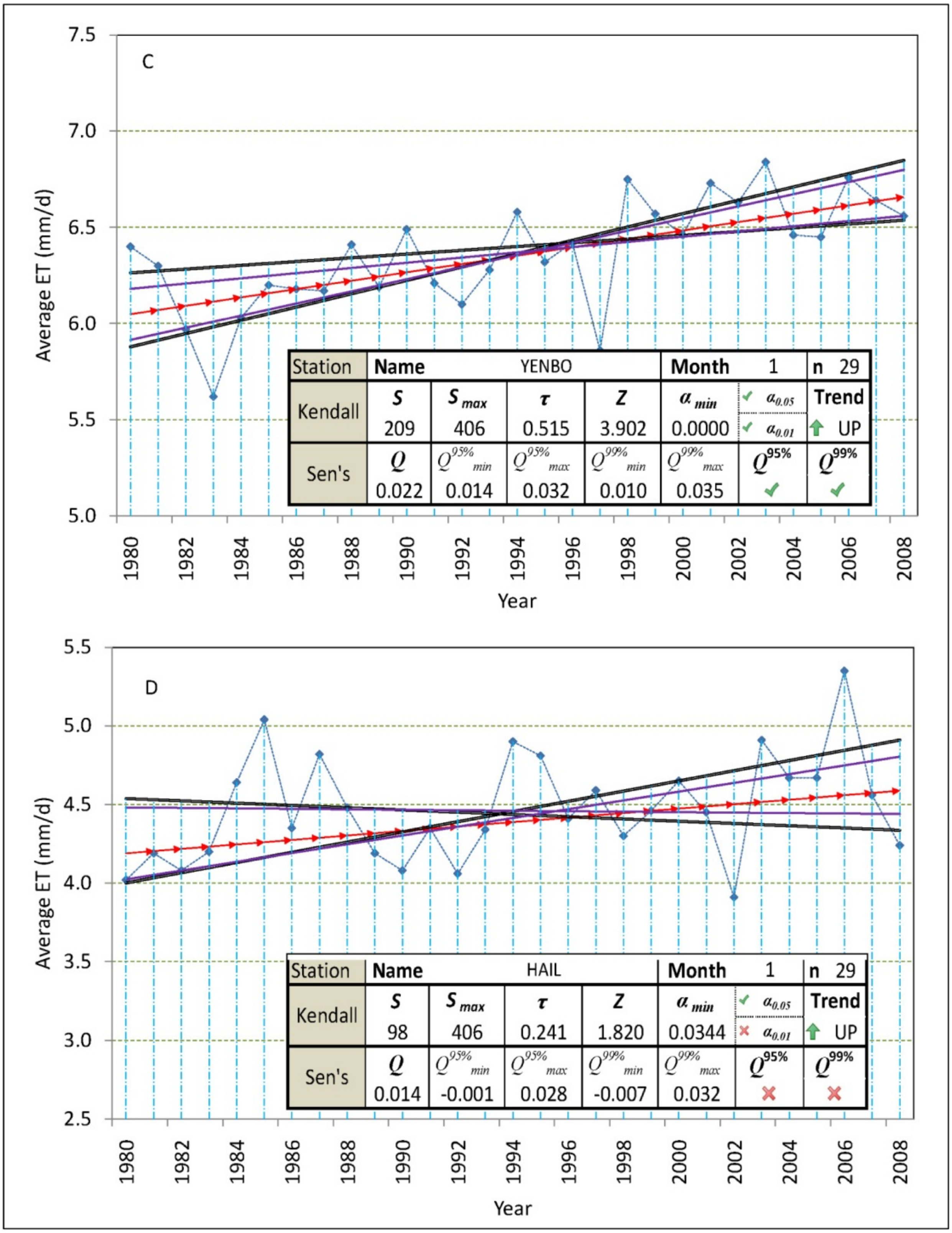

Figure 6. Analysis of monthly average ET_o trends using Mann-Kendall and Sen slope estimator and their significant tests parameters: A: Tabuk area, B: Sharurrah area, C: Yenbo area, and D: Hail area.

Figure 6A-D represents four possible cases of Q and τ and their significance. In Tabuk and Sharurrah, both Q (-0.020, -0.028) and τ (-0.365, -0.281), respectively, were negative indicating a decreasing trend for ET_o. However, this decrease is significant for Tabuk and not significant for Sharurrah at 99% probability level as confirmed by both statistical methods. In the case of Tabuk , the value of calculated α_{min} = 0.0029 is less than 0.01 indicating a significant trend according to Mann-Kendall test; for Sen slope test the 99% minimum and maximum values of the confidence interval are both negative indicating that the slope Q is not zero and therefore a negative trend is confirmed. However, for Sharurrah stations α_{min} = 0.03 is less than 0.05 but larger than 0.01 indicating that the positive trend is significant at 95% but not at 99% level according to Mann-kendall test. A slightly different result was found in Sharurrah with Sen slope test. The upper limits for the Q confidence interval at 95% and 99% were both larger than zero, $Q_{\max}^{95\%} = 0.004$, $Q_{\max}^{99\%} =$ 0.015 indicating that the median slope of the ET_o series, Q, can actually be zero and therefore the negative trend is not significant at both levels. This results show that Sen Slope test can be more conservative than Mann-Kendall test.

Both Yenbo and Hail have increasing ET_o trends, as shown in Figure 6C and D, because τ and Q values were both positive (Q= 0.022, τ= 0.515 for Yenbo; while Q= 0.01 and τ = 0.24 for Hail). Both tests showed that ET_o in Yenbo is increasing significantly at 95% as well as at 99% level since τ and Q were positive and α_{min} = 0.000 < 0.05 and $Q_{\min}^{95\%} > 0.0$. However, in Hail this uptrend was significant according to Mann-Kendall (α_{min} = 0.000 < 0.05) at 95% level but not significant according to Sen Slope since $Q_{\min}^{95\%} = -0.001$ indicating the possibility of the slope being zero. These results indicated the validity of these two statistical methods to detect trends in a time series data.

The previous analyses shown in Figure 6 were carried out for the 27 stations out of 29 under study. Man-Kendall, and Sen's methods' can deal with data series with 10 or more data points. However, Gurrayat and Dammam have less than 10 years of data and they were excluded from trend analysis. Average ET_o time series were analyzed for each month and the resultant Sen slope Q and Kendall τ are shown in Table 2 and Table 3, respectively followed by up or down arrows to indicate their significance. Up-arrows in light or dark black indicate significance up trend while similar light and dark black down arrows indicate a significant down trends at 95% and 99% probability level, respectively. Numbers without arrows are not statistically significant. The total number of stations with a decreasing or increasing trend in each month were calculated and shown at the bottom of the Table. whereas the number of months at which stations showed a decreasing or increasing trends were shown for each station at the right side of the Table. Numbers between brackets indicates the number of months or stations with the corresponding significant trend.

The tests were carried out for maximum, minimum and average monthly ET_o but only the average ET_o is shown in the Tables, because extreme ETo showed similar behavior to that of average ETo.

No	Station	Month Number												Number of months	
		1	2	3	4	5	6	7	8	9	10	11	12	Increasing	Decreasing
1	TURAIF	0.009	0.017	⬆ 0.038	0.025	⬆ 0.059	⬆ 0.064	⬆ 0.055	⬆ 0.079	↑ 0.034	↑ 0.036	0.015	0.012	12 (7)	0 (0)
2	ARAR	0.010	0.010	⬆ 0.046	↑ 0.044	⬆ 0.063	⬆ 0.099	↑ 0.089	⬆ 0.085	⬆ 0.058	⬆ 0.062	0.024	0.015	12 (8)	0 (0)
4	ALJOUF	0.009	0.016	↑ 0.025	0.032	⬆ 0.040	⬆ 0.044	↑ 0.042	⬆ 0.060	0.021	↑ 0.033	0.029	0.008	12 (6)	0 (0)
5	RAFHA	-0.018	-0.018	0.012	0.006	-0.007	0.025	0.019	-0.002	-0.018	0.009	-0.002	-0.016	5 (0)	7 (0)
6	QAISUMAH	-0.013	0.008	0.006	0.007	-0.012	⬇ -0.059	⬇ -0.090	⬇ -0.065	↓ -0.046	-0.006	-0.009	-0.021	3 (0)	9 (4)
7	TABUK	⬇ -0.020	-0.007	-0.012	-0.020	-0.005	-0.018	-0.011	0.001	↓ -0.025	-0.002	-0.010	↓ -0.021	1 (0)	11 (3)
8	HAFR AL-BATIN	0.015	↑ 0.065	⬆ 0.132	⬆ 0.139	↑ 0.119	0.094	-0.005	0.068	0.023	0.039	0.014	-0.038	10 (4)	2 (0)
9	HAIL	0.014	⬆ 0.032	⬆ 0.039	⬆ 0.049	⬆ 0.049	⬆ 0.072	⬆ 0.060	⬆ 0.074	↑ 0.047	↑ 0.035	0.020	0.017	12 (9)	0 (0)
10	WEJH	⬇ -0.016	-0.010	-0.017	-0.018	-0.016	-0.027	0.005	-0.013	-0.006	-0.008	0.004	-0.001	2 (0)	10 (1)
11	GASSIM	-0.008	↑ 0.025	0.037	↑ 0.062	0.038	⬆ 0.048	0.025	0.036	↑ 0.039	0.012	0.015	0.010	11 (4)	1 (0)
12	DHAHRAN	0.011	⬆ 0.030	⬆ 0.063	↑ 0.045	↑ 0.062	0.032	↑ 0.047	-0.026	↑ 0.030	0.020	↑ 0.026	0.009	11 (7)	1 (0)
14	AHSA	-0.018	-0.012	0.010	0.014	↓ -0.077	↓ -0.070	⬇ -0.101	↓ -0.110	↓ -0.053	⬇ -0.058	↓ -0.033	-0.014	2 (0)	10 (7)
15	MADINA	-0.011	0.016	0.005	0.024	-0.010	0.013	-0.006	0.020	0.025	-0.003	0.012	0.006	8 (0)	4 (0)
16	RIYADH (New)	-0.008	0.005	-0.002	0.050	0.020	0.021	-0.023	0.016	0.030	0.026	0.002	0.002	9 (0)	3 (0)
17	RIYADH (Old)	0.006	⬆ 0.025	0.033	0.047	⬆ 0.051	0.009	-0.003	0.006	0.026	0.013	0.005	0.010	11 (2)	1 (0)
18	YENBO	⬆ 0.022	⬆ 0.040	⬆ 0.049	⬆ 0.037	⬆ 0.058	⬆ 0.070	↑ 0.053	⬆ 0.072	⬆ 0.071	⬆ 0.050	⬆ 0.036	⬆ 0.032	12 (12)	0 (0)
19	JEDDAH	-0.001	-0.002	0.002	0.001	⬆ 0.034	↑ 0.023	⬆ 0.023	0.016	0.008	0.013	0.009	-0.006	9 (3)	3 (0)
20	MAKKAH	-0.002	0.005	0.000	-0.005	-0.002	-0.006	-0.019	-0.024	-0.023	⬇ -0.024	-0.018	-0.007	1 (0)	10 (1)
21	TAIF	0.010	⬆ 0.040	↑ 0.028	↑ 0.026	⬆ 0.046	⬆ 0.063	↑ 0.055	⬆ 0.033	⬆ 0.030	↑ 0.022	0.014	0.008	12 (9)	0 (0)
22	BAHA	↓ -0.027	-0.012	-0.015	0.017	0.013	0.020	0.000	0.008	-0.015	-0.013	-0.031	-0.021	5 (0)	7 (1)
23	W-DAWASIR	0.000	0.033	↑ 0.052	0.009	0.002	0.006	-0.026	↑ 0.033	0.014	0.013	↑ 0.029	0.012	10 (3)	1 (0)
24	BISHA	-0.001	0.018	0.017	0.024	0.023	↑ 0.037	0.020	⬆ 0.037	↑ 0.036	0.025	0.015	0.007	11 (3)	1 (0)
25	ABHA	0.000	⬆ 0.032	⬆ 0.036	⬆ 0.037	0.024	0.005	0.000	0.016	↑ 0.021	↑ 0.025	0.008	0.006	10 (5)	0 (0)
26	KHAMIS MUSHAIT	0.009	⬆ 0.028	⬆ 0.027	↑ 0.031	⬆ 0.039	↑ 0.034	0.013	⬆ 0.028	⬆ 0.035	⬆ 0.030	0.015	0.012	12 (8)	0 (0)
27	NEJRAN	-0.011	-0.004	-0.009	-0.002	-0.024	↓ -0.044	↓ -0.042	-0.032	-0.017	-0.016	-0.017	-0.007	0 (0)	12 (2)
28	SHARURRAH	-0.028	-0.044	↓ -0.052	0.008	-0.062	-0.058	↓ -0.091	-0.078	↓ -0.072	⬇ -0.081	-0.026	-0.023	1 (0)	11 (4)
29	GIZAN	0.000	0.000	0.001	0.000	-0.002	0.003	0.007	-0.006	-0.003	⬇ -0.012	-0.002	0.000	5 (0)	5 (1)
No. of stations Increasing		10 (1)	19 (9)	20 (11)	23 (9)	17 (11)	20 (10)	15 (8)	18 (9)	17 (10)	17 (8)	18 (3)	15 (1)		
No of stations Decreasing		14 (3)	8 (0)	6 (1)	4 (0)	10 (1)	7 (3)	11 (4)	9 (2)	10 (4)	10 (4)	9 (1)	11 (1)		

Symblos Key: ⬆ Increasing 99% · ↑ Increasing 95% · No trend · ↓ Decreasing 95% · ⬇ Decreasing 99%

Table 2. Monthly trends in the average ETo as estimated from Sen's slope statistics (Q) for various meteorological Station. Numbers in parenthesis indicate number of significant values.

No	Station	Month Number												Number of months	
		1	2	3	4	5	6	7	8	9	10	11	12	Increasing	Decreasing
1		0.16	↑ 0.23	⬆ 0.39	↑ 0.24	⬆ 0.38	⬆ 0.46	⬆ 0.37	⬆ 0.41	↑ 0.28	↑ 0.29	0.13	0.14	12 (9)	0 (0)
2	ARAR	0.19	0.14	⬆ 0.36	⬆ 0.32	⬆ 0.44	⬆ 0.54	⬆ 0.33	⬆ 0.40	⬆ 0.40	⬆ 0.43	↑ 0.24	0.22	12 (9)	0 (0)
4	ALJOUF	0.13	0.20	⬆ 0.33	↑ 0.22	⬆ 0.37	⬆ 0.50	⬆ 0.33	⬆ 0.48	0.21	↑ 0.30	↑ 0.26	0.12	12 (8)	0 (0)
5	RAFHA	↓ -0.24	-0.17	0.09	0.04	-0.07	0.17	0.05	-0.01	-0.14	0.08	-0.01	-0.15	5 (0)	7 (1)
6	QAISUMAH	-0.16	0.08	0.03	0.04	-0.10	⬇ -0.39	⬇ -0.46	⬇ -0.47	⬇ -0.34	-0.06	-0.06	-0.17	3 (0)	9 (4)
7	TABUK	⬇ -0.36	-0.08	-0.14	-0.20	-0.06	-0.20	-0.14	0.01	↓ -0.28	-0.02	-0.16	⬇ -0.33	1 (0)	11 (3)
8	HAFR AL-BATIN	0.09	⬆ 0.43	⬆ 0.57	⬆ 0.49	⬆ 0.43	↑ 0.32	-0.02	↑ 0.30	0.12	0.20	0.07	-0.13	10 (6)	2 (0)
9	HAIL	↑ 0.24	⬆ 0.43	⬆ 0.39	⬆ 0.40	⬆ 0.47	⬆ 0.50	⬆ 0.44	⬆ 0.57	⬆ 0.33	↑ 0.28	0.15	0.22	12 (10)	0 (0)
10	WEJH	⬇ -0.31	-0.16	↓ -0.23	-0.20	-0.18	-0.16	0.12	-0.10	-0.03	-0.12	0.07	-0.01	2 (0)	10 (2)
11	GASSIM	-0.10	↑ 0.29	↑ 0.25	⬆ 0.32	↑ 0.23	⬆ 0.39	0.16	↑ 0.24	↑ 0.28	0.13	0.14	0.10	11 (7)	1 (0)
12	DHAHRAN	0.17	⬆ 0.38	⬆ 0.47	⬆ 0.32	⬆ 0.32	0.21	↑ 0.27	-0.18	⬆ 0.33	0.21	⬆ 0.35	0.17	11 (7)	1 (0)
14	AHSA	-0.22	-0.12	0.04	0.13	⬇ -0.35	↓ -0.32	⬇ -0.38	⬇ -0.36	⬇ -0.35	⬇ -0.44	⬇ -0.39	-0.13	2 (0)	10 (7)
15	MADINA	-0.17	0.12	0.10	0.15	-0.06	0.09	-0.06	0.12	↑ 0.24	-0.05	0.15	0.08	8 (1)	4 (0)
16	RIYADH (New)	-0.10	0.07	-0.01	0.22	0.14	0.12	-0.18	0.18	0.24	0.19	0.01	0.04	9 (0)	3 (0)
17	RIYADH (Old)	0.13	⬆ 0.35	↑ 0.25	↑ 0.22	⬆ 0.43	0.10	-0.05	0.06	0.20	0.13	0.06	0.11	11 (4)	1 (0)
18	YENBO	⬆ 0.51	⬆ 0.41	⬆ 0.47	⬆ 0.39	⬆ 0.41	⬆ 0.43	⬆ 0.33	⬆ 0.40	⬆ 0.48	⬆ 0.51	⬆ 0.38	⬆ 0.41	12 (12)	0 (0)
19	JEDDAH	-0.02	-0.04	0.03	0.03	⬆ 0.39	↑ 0.31	⬆ 0.39	0.21	0.10	0.16	0.11	-0.10	9 (3)	3 (0)
20	MAKKAH	-0.04	0.05	0.00	-0.05	-0.03	-0.06	-0.18	↓ -0.28	↓ -0.26	⬇ -0.41	-0.21	-0.11	2 (0)	10 (3)
21	TAIF	0.18	⬆ 0.55	⬆ 0.32	↑ 0.31	⬆ 0.36	⬆ 0.41	↑ 0.29	⬆ 0.36	⬆ 0.38	↑ 0.31	↑ 0.23	0.13	12 (10)	0 (0)
22	BAHA	⬇ -0.38	-0.11	-0.10	0.11	0.11	0.19	0.00	0.10	-0.09	-0.12	-0.21	-0.18	4 (0)	7 (1)
23	W-DAWASIR	0.02	↑ 0.27	↑ 0.34	0.06	0.01	0.04	-0.14	⬆ 0.35	0.08	0.17	↑ 0.32	0.10	11 (4)	1 (0)
24	BISHA	-0.03	0.21	0.14	0.14	0.18	⬆ 0.34	0.15	⬆ 0.34	↑ 0.29	0.21	0.16	0.13	11 (3)	1 (0)
25	ABHA	0.00	⬆ 0.46	⬆ 0.35	⬆ 0.35	↑ 0.25	0.05	0.00	0.21	↑ 0.28	⬆ 0.31	0.19	0.11	11 (6)	1 (0)
26	KHAMIS MUSHAIT	0.13	⬆ 0.35	⬆ 0.40	⬆ 0.33	⬆ 0.35	↑ 0.31	0.14	⬆ 0.42	⬆ 0.38	⬆ 0.36	0.22	0.15	12 (8)	0 (0)
27	NEJRAN	-0.18	-0.05	-0.11	-0.04	-0.18	⬇ -0.32	↓ -0.31	↓ -0.22	-0.15	-0.12	↓ -0.25	-0.09	0 (0)	12 (4)
28	SHARURRAH	↓ -0.28	↓ -0.26	⬇ -0.36	0.04	↓ -0.25	↓ -0.27	⬇ -0.36	↓ -0.28	⬇ -0.37	⬇ -0.41	-0.16	-0.21	1 (0)	11 (9)
29	GIZAN	0.01	0.01	0.03	0.01	-0.04	0.04	0.10	-0.10	-0.07	↓ -0.29	-0.03	0.00	6 (0)	5 (1)
No. of stations Increasing		13 (2)	19 (11)	21 (13)	23 (12)	17 (13)	20 (11)	14 (8)	18 (11)	17 (11)	17 (8)	18 (6)	15 (1)		
No of stations Decreasing		14 (5)	8 (1)	6 (2)	4 (0)	10 (2)	7 (4)	12 (4)	9 (5)	10 (5)	10 (4)	9 (2)	11 (1)		

Symblos Key:	⬆ Increasing 99%	↑ Increasing 95%	No trend	↓ Decreasing 95%	⬇ Decreasing 99%

Table 3. Monthly trends in the Average ETo as estimated from Mann-kendall statistics (τ) for various meteorological Station. Numbers in parenthesis indicate number of significant values.

Fourteen stations have a positive Q and τ, for at least 10 months in a year therefore an uptrend in ETo namely; Turaif, Arar, Al jouf, Hafr Al-Baten, Hail, Gassim, Dhahran, Riyadh (old), Yenbo, Taif, W-dawaser, Bisha, Abha, and khamis Mushait. Another six stations showed a negative or zero Q during the whole year, therefore a downtrend in ET_oincluding; Tabuk, Wejh, Makkah, Nejran, Sharurrah, and Gizan. The other seven stations showed a mix of increasing and decreasing trends during the year and those are Rafha, Qaisumah, Ahsa, Madina, Riyadh (new), Jeddah, and Baha.

However, the up or down trends or downtrends in ET_o in the first mentioned group were not always significant as indicated by the upward arrows and summed in the last two columns of Tables 2 and 3. Only Yenbo had a confirmed significant trend at 95% level during the entire year. Other stations showed a significant up trends in ET_o for several months during the year including Hail and Taif , 10 months; Turaif and Arar, 9 months; Al jouf and Khamis Mushait, 8 months. The other stations among the uptrend group had significant uptrend in 3 months to 7 months in a year as shown in Table 2.

The number of stations with a decreasing trend is far less than those with increasing ET_o. Few stations showed a decreasing trend in ET_o for 9 months or higher including, Qaisumah, Tabuk, Wejh, Ahsa, Makkah, Nijran and Sharurrah. However, only Ahsa station had a significant decreasing trend for 7 months followed by Qaisumah and Sharurrah, 4 months, and Tabuk with only 3 months of declining in ET_o. The rest of stations, Wejh, Makkah, Nejran, Gizan, had a decreasing trend but this trend is not significant at 95% probability level.

The numbers of stations with increasing or decreasing trend are shown in the last two rows of Table 2 and 3. Figure 7, as well, illustrates the number of stations with significant/non-significant increasing/decreasing trend of ET throughout the studied areas. At least 15 stations or higher showed an increasing trend for the entire year except in January at which 14 stations showed a decreasing trend. March, April and June showed the highest number of stations with increasing ET_o. However, the significant increase in ET_o were confirmed for about 10 stations and for 9 months, February to October. During the months of October to January about 10 stations showed a decreasing trend but this decrease was significant for only 4 stations in September and October, one station in November and December and 3 stations in January.

Further inspection on the location of stations with increasing trends in ET_o revealed that most of these stations are located in the northern part of the Arabian peninsula north to the latitude line of 22 degrees. However, some other stations were located southern of this line at the southern west corner of Saudi Arabia. It seemed that stations located along the longitudinal line of 45 degrees showed an increasing trend. Actually the wind direction over the Arabian peninsula seemed to follow this line from south west to north in rainy seasons and from north to south west in the dry seasons.

To have an aerial graph for the regions with a decreasing or increasing trend in ET_o a contour map were plotted for each months and the results are shown in Figure 8. Certainly, regions with increasing trends are concentrated in the northern part of Saudi Arabia and extended to the south along the 45-degree longitudinal line. Significant and increasing regions, indicated by black and grey regions (P>95%) are prevail for most of the year except in January and July to some extent. In January most of SA areas have decreasing *ETo* as shown in Figure 8 and also in Table 3 where 14 stations have a decreasing trends; although this decrease is not significant at 95% level except for 3 stations. The southeastern parts seemed to have decreasing trends most of the years, but also this trend is not significant at 95% except in July and October as indicated by the darker dotted regions.

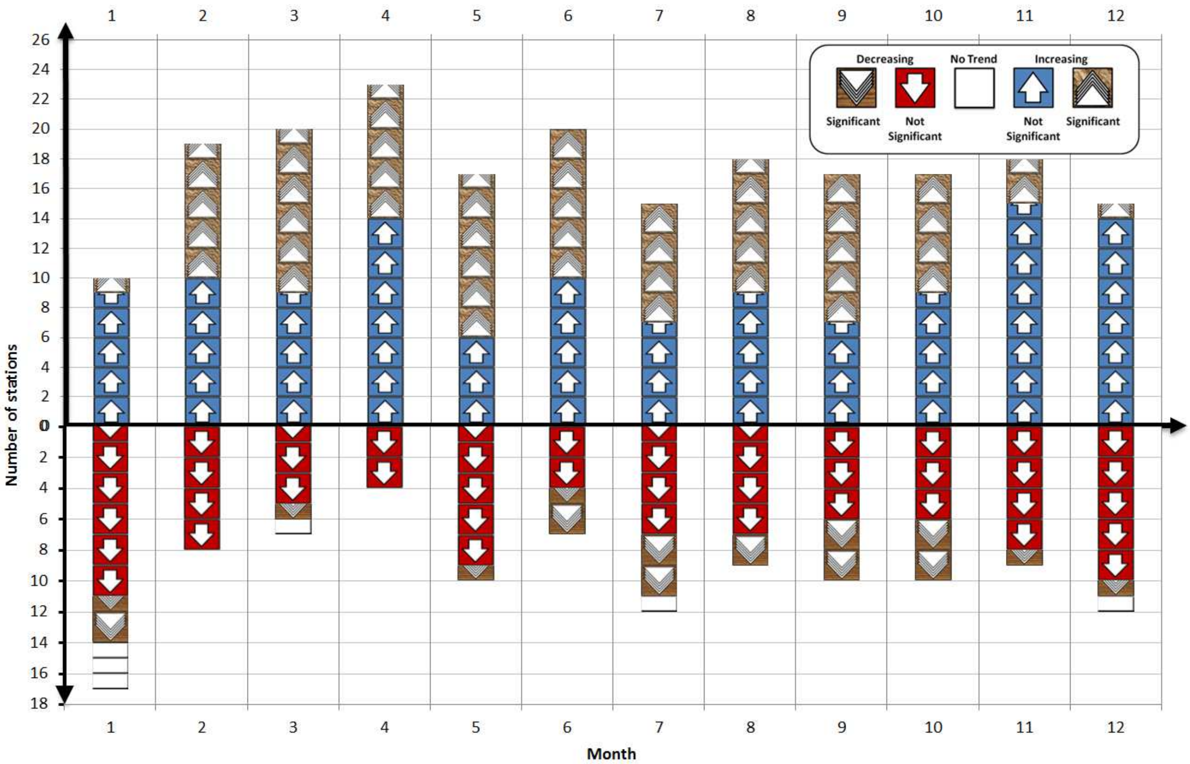

Figure 7. Number of stations with significant/non-significant increasing/decreasing trends of ET in the studied areas.

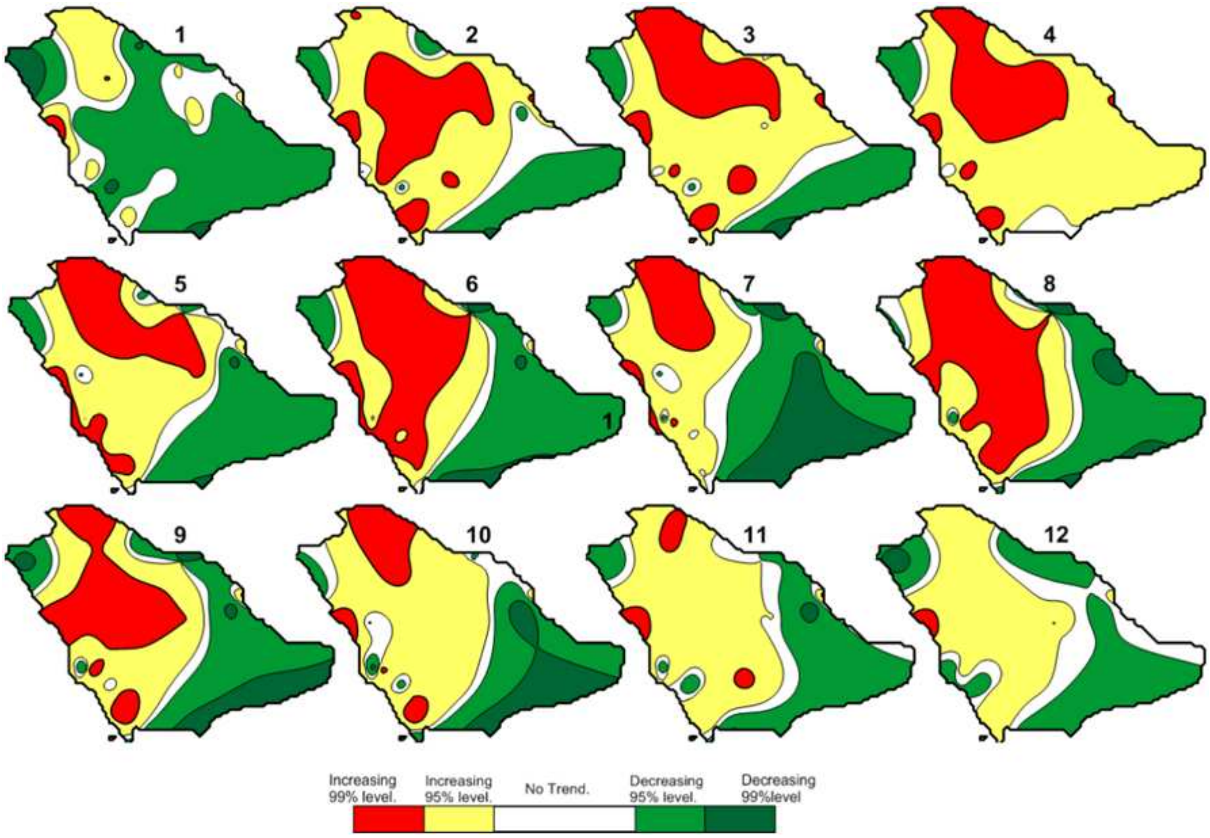

Figure 8. Contour plots showing the distribution ETo trends' direction and confidence level over the area of KSA.

4. Conclusion

Water scarcity problem can be solved by proper management of water usage. Most of the depleted water in KSA is consumed through agriculture. Identifying the ET_o trend and knowing the zones having the least ET_o values can help in determining the future plans of agricultural and water extensions. Historical analysis of daily ET_o in Saudi Arabia was carried out using Penman Monteith equation (FAO-56) for 29 meteorological stations distributed all over Saudi Arabia for the period 1980 to 2008. The long time average daily ET_o varied from about 5 mm/d in Jan to 15 mm/day in July which is one of the hottest months in the country. ET_o time series analysis using Mann-Kendall and Sen slope statistics revealed that ET_o has been increasing steadily during the study period. The average minimum and maximum daily ET_o increased steadily and ET_o average increased from about 9.6 to about 10.4 mm/day in 2008. Trend analysis revealed that about 14 of the weather stations showed a significant increasing trend in ET_o during the year for more than 7 months. Only 4 stations showed decreasing trends in three months, September, October and January.

Increasing ET_o trends prevail in the northern and south-west areas along the longitudinal line of 45 degrees while decreasing trends prevail in the north western spot along the red sea and south eastern parts along the Arabian Gulf. This demonstrates that ET_o fluctuation is increasing with time that can be considered a significant sign for climate variability in the

Arabian peninsula. This increase in ET_o seemed to be mainly affected by the global warming or the increase in temperature in the Arabian peninsula which was confirmed by several studies mentioned in this paper. Analyses of longer historic data are needed to confirm these findings. This demonstrates that ET_o fluctuation is increasing with time that can be considered a significant sign for climate change. Though, the findings of this research suggest the needs to consider ET_o changes in the planning for agricultural and water resources projects. Thus to rank the areas with fixed and decreasing ET_o trend as highly recommended zones for future agricultural projects, and to do the opposite with the increasing ETo trends' zones. Finally, if the low ranked zones are essential due to other circumstances, then the water management policy should consider the increment rate in ETo and its effect on water consumption.

Author details

Mohammad Elnesr* and Abdurrahman Alazba
King Saud University, Alamoudi Water Chair, Saudi Arabia

Acknowledgement

The authors wish to express their deep thanks and gratitude to "Shaikh Mohammad Bin Husain Alamoudi" for his kind financial support to the King Saud University, through the research chair "Alamoudi Chair for Water Researches" (AWC), where this paper is part of the AWC chair activities. Thanks should also be expressed to the Presidency of Meteorology and Environment in Riyadh, KSA, who kindly support this research my meteorological data.

5. References

Abderrahman W. A. ; Bader T. A. ; Asfahan Ullah Kahn ; Ajward M. H. (1991) Weather Modification Impact on Reference Evapotranspiration, Soil Salinity and Desertification in Arid Regions, A Case Study. J. Arid Environments. 20(3):277-286

Abderrahman, W. A. (2001) Water demand management in Saudi Arabia. Ch. 6 In: Water Management In Islam proc.. IDRC/UNU Press 2001 [Naser I. Faruqui, Asit K. Biswas, and Murad J. Bino (eds.)]. 170 pp. available online at: http://www.idrc.ca/en/ev-93954-201-1-DO_TOPIC.html

Abdreeahman, W.A., and Al-Harazin, I. M. (2003). The impacts of global climatic change on reference crop evapotranspiration, irrigation water demands, soil salinity, and desertification in Arabian Peninsula. 67:74p. In Proc. Intl. Conf. of "Desertification in the Third Millennium". Dubai, 12-15 February 2003. Ed. Alsharhan, A. S. Organized by Zayed International Prize for the Environment. 504 pp

* Corresponding Author

Abo-Ghobar, H. (2000). Estimation of reference evapotranspiration for southern region of Saudi Arabia. Irrig Sci 19: 81 - 86.

Abramowitz, M., Stegun, I. eds. (1972), Handbook of Mathematical Functions with Formulas, Graphs, and Mathematical Tables, New York: Dover Publications

Al-Ansari, N., E. Salameh and H. Al-Omari, (1999). Analysis of rainfall in the badia region, Jordan. Research Paper No. 1, Al-al-Bayt University, Jordan.

Albakry, A., Alsaleem, I., and ElBeishi, M. (2010). Geography of the Kingdom of Saudi Arabia and Some Other Countries. 3rd ED. ISBN: 9960-19-056-0, Pub. Saudi Ministry of Education.(www.moe.gov.sa) 164pp.

Allen, R. G., Pereira, L. S., Raes, D., Smith, M., (1998). Crop evapotranspiration. Guidelines for computing crop water requirements. FAO Irrigation and drainage paper 56. Food and Agriculture Organization of the United Nations, 300pp.

Allen, R.G., Walter, I.A., Elliott, R.L., Howell, T.A., Itenfisu, D., Jensen, M.E. and Snyder, R.L. (2005). The ASCE Standardized Reference Evapotranspiration Equation. Amer. Soc. of Civil Eng. Reston, Virginia. 192pp.

AQUASTAT. (2008). FAO's Information System on Water and Agriculture, Climate information tool. Website, http://www.fao.org/nr/water/aquastat/ countries/saudi_ arabia/index.stm., accessed 25/2/2009.

Bandyopadhyay, A., A. Bhadra, N. S. Raghuwanshi, and R. Singh. (2009). Temporal trends in estimates of reference evapotranspiration over india. Journal of Hydrologic Engineering 14(5):508-515.

Burman, R.D., Jensen M.E. and Allen R.G. (1987). Thermodynamic factors in evapotranspiration. In: Proc. Irrig. and Drain. Spec. Conf., James L.G. and English M.J. (eds). ASCE, Portland, Ore., July. : 28-30.

Cohen, S. and Stanhill G. (1996). Contemporary climate change in Jordan Valley. J. Appl. Meteorol., 35: 1051-1058.

Dinpashoh, Y., (2006). Study of reference crop evapotranspiration in I.R. of Iran. Agric. Water Manage. 84: 123–129.

Doorenbos, J. and Pruitt, W. O. (1975). Guidelines for predicting crop water requirements, Irrigation and Drainage Paper 24, Food and Agriculture Organization of the United Nations, Rome, 179 p.

Elnesr, M., & Alazba, A. (2010). Spatio-Temporal Variability of Evapotranspiration over the Kingdom of Saudi Arabia. Applied Engineering in Agriculture, ASABE, 26(5), 833-842.

Elnesr, M., A. Alazba and M. Abu-Zreig, (2010a). Analysis of evapotranspiration variability and trends in the Arabian Peninsula. Am. J. Environ Sci., 6: 535-547. DOI: 10.3844/ajessp.2010.535.547
URL: http://www.thescipub.com/abstract/10.3844/ajessp.2010.535.547

Elnesr, M., M.M. Abu-Zreig and A.A. Alazba, (2010b). Temperature Trends and Distribution in the Arabian Peninsula. Am. J. Environ. Sci., 6: 191-203. DOI: 10.3844/ajessp.2010.191.203
URL: http://www.thescipub.com/abstract/10.3844/ajessp.2010.191.203

Fehrman r. L. (2007). Increasing Evapotranspiration Trends over the Mississippi River Basin. MSc. Thesis. faculty of the graduate school of Cornell Univ.

FU, G. , Stephen, C. P. , YU, J. (2009). A critical overview of pan evaporation trends over the last 50 years. Climatic change 97(1-2):193-214

Gao, G., D. Chen, C.-y. Xu, and E. Simelton. (2007). Trend of estimated actual evapotranspiration over china during 1960–2002. Journal of Geophysical Research 112(D11):D11120+.

Garbrecht, J., Van Liew, M., and Brown, G. O. (2004). Trends in precipitation, streamflow, and evapotranspiration in the great plains of the united states. Journal of Hydrologic Engineering 9:360-367.

Hakan A., Savaş K., Osman Ş. (2010). Trend Analysis of Hydrometeorological Parameters in Climate Regions of Turkey. Conference prerelease, BALWOIS 2010 – Ohrid, Republic of Macedonia –25, 29 May 2010 URL: www.balwois.com/balwois/administration/full_paper/ffp-1457.pdf accessed 27/3/2010

Harrison, L. P. (1963). Fundamentals concepts and definitions relating to humidity. In Wexler, A (Editor) Humidity and moisture Vol 3, Reinhold Publishing Co., N.Y.

Hegerl, G.C., F. W. Zwiers, P. Braconnot, N.P. Gillett, Y. Luo, J.A. Marengo Orsini, N. Nicholls, J.E. Penner and P.A. Stott. (2007). Understanding and Attributing Climate Change. In: Climate Change 2007: The Physical Science Basis. Contribution of Working Group I to the Fourth Assessment Report of the Intergovernmental Panel on Climate Change [Solomon, et al. (eds.)]. Cambridge University Press, Cambridge, United Kingdom and New York, NY, USA. 690pp.

Hobbins, M. T., Ramı´rez, J. A., Brown, T. C. (2004). Trends in pan evaporation and actual evapotranspiration across the conterminous U.S.: Paradoxical or complementary? Geophysical Research Letters. 31(13): L13503+

Isaaks E. H., and Srivastava R. M. (1989). An Introduction to Applied Geostatistics. Oxford University Press. 198 Madison Av. NY: 279-330. 560pp.

Kendall M., and Gibbons J.D., (1990). Rank Correlation Methods. New York: Oxford University Press, fifth ed. 272pp.

Liu, B., M. Xu, M. Henderson, and W. Gong. (2004). A spatial analysis of pan evaporation trends in china, 1955–2000. Journal of Geophysical Research 109(D15):D15102+.

Milly, P.C.D., and Dunne K.A., (2001). Trends in evaporation and surface cooling in the Mississippi River basin. Geophys. Res. Lett., 28, 1219-1222.

MOMRA (2007). Ministry of Municipal and Rural Affairs map of Saudi districts. (official website) URL: http://www.momra.gov.sa/GeneralServ/mun/imap.htm, accessed Dec. 2009.

Murray F.W. (1967). On the computation of saturation vapor pressure. J. Appl. Meteor. 6: 203-204.

Mustafa M. A., Akabawi K. A. and Zoghet M. F. (1989). Estimation of Reference Crop Evapotranspiration for the Life Zones of Saudi Arabia. J. Arid Environ. 17: 293-300.

Myneni, R.B., C.D. Keeling, C.J. Tucker, G. Asrar, Nemani R.R., (1997). Increased plant growth in the northern high latitudes from 1981 to 1991. Nature, 386: 698-702.

NIMA (2003). National Imagery and Mapping Agency. The United States Government. No copyrights under Title 17 U.S.C.

Roderick, M.L. and Farquhar, G.D. (2004). Changes in Australian pan evaporation from 1970 to 2002. Intl. J. of Climatology 24: 1077-1090.

Schwartz, P. and Randall D. (2003). An abrupt climate change scenario and its implications for United States national security. Global Business Network, Emeryville, CA. Online source: www.edf.org/documents/3566_AbruptClimateChange.pdf. 22pp.

Sen, P.K., 1968. Estimates of the regression coefficient based on Kendall's τ. Journal of the American Statistical Association. 63:1379-1389 quoted from Brauner, S. (1997) Nonparametric Estimation of Slope: Sen's Method in Environmental Pollution. In The Environmental Sampling & Monitoring Primer Project. Ed. Gallagher D. Online: http:// www.cee.vt.edu /ewr/environmental/teach/smprimer/Sen/Sen.html.

Shenbin, C., Yunfeng, L., and Thomas, A. (2006). Climatic Change on The Tibetan Plateau: Potential Evapotranspiration Trends From 1961–2000 Climatic Change 76: 291–319

Smadi M., (2006). Observed Abrupt Changes in Minimum and Maximum Temperatures in Jordan in the 20th Century. Am. J. Environ. Sci., 2 (3): 114-120.

Smadi, M.M. and Zghoul, A., (2006). A Sudden Change In Rainfall Characteristics In Amman, Jordan During The Mid 1950s. Am. J. of Environ. Sci. 2 (3): 84-91.

Song, Z. W., H. L. Zhang, R. L. Snyder, F. E. Anderson, and F. Chen. (2010). Distribution and trends in reference evapotranspiration in the north china plain. Journal of Irrigation and Drainage Engineering 136(4):240-247.

Surfer (2002). Surfer©, a surface mapping system. Windows™ Software. Golden Software Inc. URL: www.goldensoftware.com

Szilagyi J. (2001). Modeled Areal Evaporation Trends Over The Conterminous United States. J. Irrig. Drain. Eng. 127(4): 196-200.

Tebakari, T., J. Yoshitani, and C. Suvanpimol. (2005). Time-space trend analysis in pan evaporation over kingdom of Thailand. J. of Hydr. Eng. 10(3):205-215.

Tetens, O. 1930. Uber einige meteorologische begriffe. Z. Geophys. 6:297-309. quoted from FAO, 1990.

Thomas, A. (2000). Spatial And Temporal Characteristics Of Potential Evapotranspiration Trends Over China. Int. J. Climatol. 20: 381–396

Wynbrandt, J. (2004). A Brief History of Saudi Arabia. Facts on File, Inc. ISBN 0-8160-5203-4. 352pp